DESIGN, FABRICATION AND CHARACTERISATION OF AN InP RESONANT TUNNELLING BIPOLAR TRANSISTOR WITH DOUBLE HETEROJUNCTIONS

M. Wintrebert-Fouquet

Physics Department, Macquarie University, NSW 2109, Australia

email: mariew@ics.mq.edu.au

ABSTRACT

An InP/$In_{0.53}Ga_{0.47}As$ resonant tunnelling bipolar transistor with double heterojunction grown by molecular beam epitaxy and fabricated by selective wet chemical etching is presented. An $In_{0.53}Ga_{0.47}As$/AlAs resonant tunnelling diode which achieves a current density of 15 kA/cm^2 at a peak voltage of 1.6 V for a peak-to-valley ratio of 39:1 is integrated at the emitter of a double heterojunction InGaAs/InP bipolar transistor. Results are presented for 3 μm × 3 μm emitter size integrated device. A negative differential shape due to the resonant tunnelling effect at the emitter controlled by a 3.4 μA base current is observed in the common-emitter current-voltage characteristics at room temperature with a current density of 9.2 kA/cm^2 and a peak-to-valley ratio of 12:1. The maximum current gain of the device is 220. However beyond the resonant tunnelling peak, the resonant tunnelling transistor presents a bistability where the collector current collapses dramatically, the transistor characteristics are recovered by increasing the collector-emitter voltage.

1. INTRODUCTION

Having successfully modelled, designed and built practical resonant tunnelling diodes (RTDs) in our previous project [1][2], we sought to use these as a base for the development of resonant tunnelling bipolar transistors (RTBTs), which are more versatile and useful devices for circuit design [3]–[6]. The RTBT is an RTD integrated with an n-p-n double heterojunction bipolar transistor (DHBT). $In_{0.53}Ga_{0.47}As$/AlAs materials for RTDs have a switching-time performance of less than 5 ps and are kept in the RTD design of our RTBT. On a lattice-matched substrate, InGaAs and AlAs have been used to demonstrate the resonant tunneling phenomenon in a very thin double barrier (DB) structure on the top of an InGaAs/InP DHBT. The best simulated current density at the peak and high peak-valley-ratio have been obtained when designing the RTD with two lightly doped InGaAs layers of 1.7 nm (emitter side) and 2.9 nm (base side) respectively sandwiching the DB. The undoped DB includes two AlAs barriers of 1.1 nm and an InGaAs well of 4.1 nm thickness. We report on the design, fabrication and characterisation of an InGaAs/AlAs Resonant Tunneling InGaAs/InP Bipolar Transistor (RTBT) on MBE-grown InP substrate. The combination of RTDs with HBTs allows us to achieve a negative differential resistance plus gain.

2. DESIGN AND FABRICATION

The RTBT epitaxial structure was built on a semi-insulating InP substrate by molecular beam epitaxy. Silicon, Beryllium and Iron are used as in the n-, p- and substrate-dopant respectively. The details of the epitaxial profile are shown on Table I, the RTD structure was grown on the top of the DHBT structure. The emitter contact of the RTBT is taken from the top part of the substrate (the RTD cap layer).
Fabrication employed a non-self-aligned triple mesa process. The emitter, base and collector are formed

0-7803-7571-8/02/$17.00 ©2002 IEEE

using highly selective wet-chemical etching. Ohmic contacts on RTD cap layer and sub-collector layer consist of non-alloyed Ni/Ge/Au and the non-alloyed base ohmic contact is in Cr/Au. The device is passivated with SiO_2. Interconnected metal is Ti/Au.
The devices were probed directly using a Cascade Microtech air coplanar microprobe and analyzed with a HP 4145B semiconductor parameter analyzer at room temperature.

TABLE I: MBE EPITAXIAL LAYERS OF THE (RTD/HBT) RTBT

Layers	Material	Doping (cm^{-3})	Thickness in nm
cap	n^+ InAs	7.0×10^{18}	30
(RTD)	n^+ InGaAs → InAs	7.0×10^{18}	20
↓			
	n^+ InGaAs	7.0×10^{18}	50
	n InGaAs	$2.0 - 7.0 \times 10^{18}$	20
	n InGaAs	1.0×10^{18}	30
buffer	InGaAs	undoped	1.7
barrier	AlAs	undoped	1.1
well	InGaAs	undoped	4.1
barrier	AlAs	undoped	1.1
buffer	InGaAs	undoped	2.9
	n InGaAs	1.0×10^{18}	30
	n InGaAs	$2.0 - 5.0 \times 10^{18}$	10
(DHBT)	n^+ InP	7.0×10^{18}	5
↓	n^+ InGaAs	7.0×10^{18}	45
	n^+ InP	7.0×10^{18}	10
	n^- InP	5×10^{17}	40
	n^- InGaAs	1.0×10^{18}	10
base	p^+ InGaAs	3×10^{19}	80
mid-collector	n^- InGaAs	undoped	20
collector	n^- InP	2×10^{16}	500
Sub-collector	n^+ InP	7.0×10^{18}	600
InP semi-insulated substrate			

3. EXPERIMENTAL RESULTS

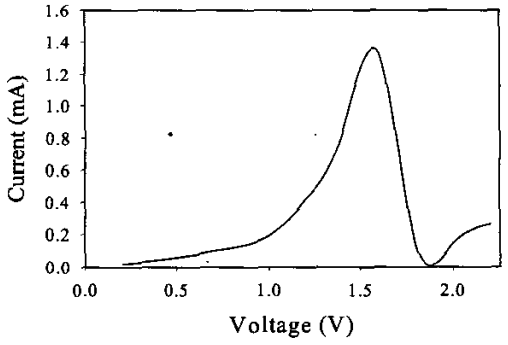

Figure 1. *I–V* characteristics of the $In_{0.53}Ga_{0.47}As$/AlAs resonant tunneling diode.

Figure 1 illustrates the *I–V* measurements of the RTD part structure with a 3 μm × 3 μm emitter size. The RTD has a current density of 15 kA/cm^2 at a voltage peak of 1.6 V with a peak-to-valley ratio (PVR) of 39:1.

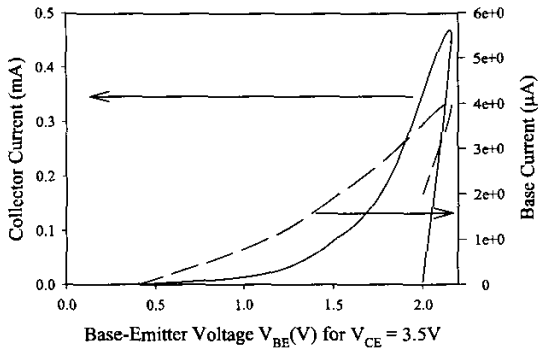

Figure 2. Common-emitter collector and base currents as functions of the base-to-emitter voltage, V_{BE}, with a constant collector-to-emitter voltage of 3.5 V.

This result can be compared with the best thin $In_{0.53}Ga_{0.47}As$/AlAs RTD layers presented by Broekaert and Fonstad [8] and Shimizu et al [9], as the current density is twenty time smaller for a PVR that is one order higher. Fig. 2 shows the common-emitter transfer characteristics. The collector current I_C and base current I_B are shown as a function of the base-to-emitter voltage V_{BE} with a constant collector-to-emitter voltage V_{CE} beyond the peak voltage of 3.5 V. The room temperature common-emitter RTBT curves are shown in Fig.3 (a) and (b). In Fig.3 (a), for low I_B, the emitter current is less than the resonant tunneling peak and the RTBT shows typical common-emitter I–V characteristics of a transistor. In Fig.3 (b) a 220 current gain is obtain for I_B = 2.6 μA and the emitter current reaches the resonant tunneling peak for I_B = 3.4 μA. Although these characteristics appear similar to those presented in [10], beyond the resonant tunneling peak for I_B > 3.4 μA, the collector current collapses dramatically down to few μA.

A method was found to re-establish the collector current in the device and recover same common-emitter I–V characteristics. This method consisted of running a set of measurements biasing the RTBT up to V_{CE} = 6 V and fixing the compliance (as a collector current limit) of the HP 4145B of 50 nA to protect the device.

4. CONCLUSION

In summary, we have demonstrated a negative differential resistance in the RTBT. For a low I_B current of 3.4 μA the RTBT starts tunneling: a PVR of 12:1 is found for a current density at the peak of 9.2 kA/cm^2. The RTBT presents bistability beyond tunneling. Further investigations are necessary to clarify the exact nature of the collapse of collector current after resonant tunneling behavior of the RTBT device. These device topologies were designed to give appropriate characteristics for the development of high speed analog-to-digital converters. RTBTs fabricated using these designs were experimentally verified to produce the transfer characteristics predicted by theory. However as the design was push towards thinner barriers in the quantum well, a bistability was observed beyond the tunnellling effect. This could be due to trapping and de-trapping of the electrons in the quantum well; a transversal conduction in the well may be possible. Others authors reported bistability in double-barrier heterostructures. B. A. Glavin et al reported theoretically the phenomenon of the formation of patterns transverse to the tunneling current [11]. P.H. Beton et al investigated the edge effects in a gated sub-micron resonant tunneling diode [12] and showed that the voltage drop across the barriers is not necessary uniform across the lateral extend of the device. The implications of a small RTD diameter with various barrier-thickness asymetries for conventional resonant-tunnelling applications were addressed in details [13] and demonstrated weak electron accumulation in the quantum well.

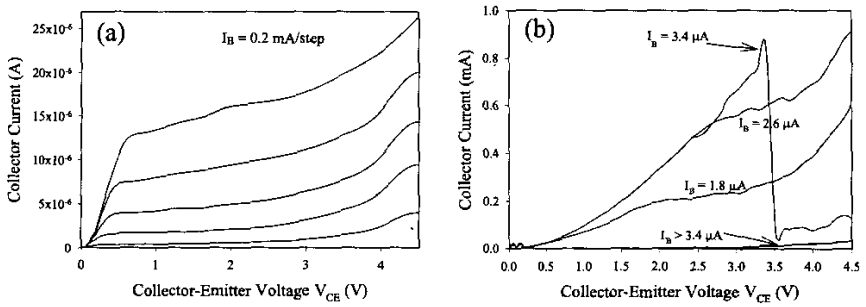

Figure 3. Common-emitter current-voltage characteristics of the RTBT with the base current of (a) $I_B = 0.2$ μA/step, (b) $I_B = 0.8$ μA/step starting from $I_B = 1.8$ μA.

ACKNOWLEDGEMENTS

The author would like to acknowledge the support of the Australian Research Council through a Large ARC grant. The author wish to thank A. Parker, J. Harrison, M. Batty, E. Goldys, S. Butcher, and T. Tansley from the division of ICS, Macquarie University, Australia, for helpful discussions.

REFERENCES

1. C.S.Y. Leung, D.J. Skellern, *1996 Conference on Optoelectronics and Microelectronic Materials and Devices Proceedings* (cat. No.96TH8197) IEEE, 267(1996).
2. C.S.Y. Leung, D.J. Skellern, *1996 Conference on Optoelectronics and Microelectronic Materials and Devices Proceedings* (cat. No. 96TH8197) IEEE, 263 (1996).
3. P. Mazumder et al, Proceedings of IEEE, **96**, No. 4, Apr. 98, 664 (1998).
4. T. P. E. Broekaert, IEEE J. Solid St. Circuits, **33**, No. 9, 1342 (1998).
5. G. I. Haddad and P. Mazumder, Solid-St. Electronics, **41**, No. 10, 1515, (1997).
6. 5. A. Seabaugh and R. Lake, Encyclopedia of Applied Physics, **22**, 335 (1998).
7. C.S.Y. Leung, M. Wintrebert-Fouquet, D.J. Skellern, *1998 Conference on Optoelectronics and Microelectronic Materials and Devices Proceedings* (cat. No.98Ex140) IEEE, 144, (1999).
8. T. P. E. Broekaert and C. G. Fonstad, Appl. Phys. **68**, 4310 (1990).
9. N. Shimizu et al, Electron. Lett. **31**, 1695, (1995).
10. A. C. Seabeaugh et al, IEEE Electron Device Lett., **14**, no. 10, 472, (1993).
11. B. A. Glavin, V.A. Kochelap, and V.V. Mitin, Phys. Rev. B. **56**, 20, 13346 (1997).
12. P.H. Peton et al, Appl. Phys. Lett., **60**, 20, 2509 (1992).
13. T. Schmidt et al, Appl. Phys. Lett., **68**, 6, 838 (1996).